Tropical Performance of HadGAM1

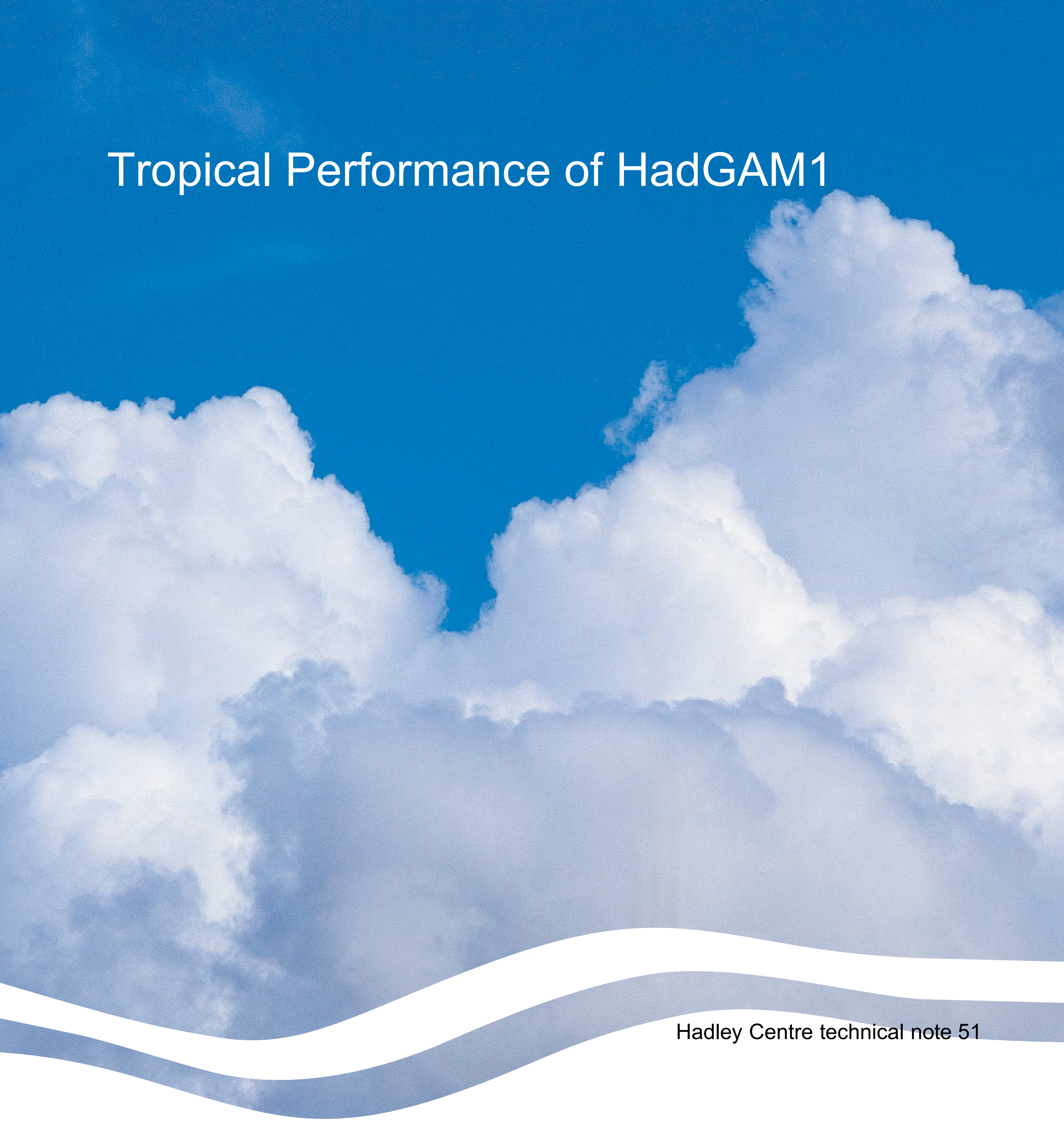

Hadley Centre technical note 51

Gill Martin, Pete Inness, Gui-Ying Yang, Brian Hoskins
Julia Slingo

23 September 2004

Tropical Performance of HadGAM1

Gill Martin[1], Pete Inness[2], Gui-Ying Yang[2], Brian Hoskins[2], Julia Slingo[2]
[1] Met Office, Fitzroy Road, Exeter EX1 3PB
[2]CGAM, University of Reading, Earley Gate, Reading
September 2003

1. Introduction

One of the most stringent tests of a general circulation model (GCM) is its ability to simulate a realistic tropical climate. This includes both the mean climate and its many modes and timescales of variability. In the following sections we examine the tropical performance of the atmosphere-only version of the new Hadley Centre climate model, HadGAM1 (*Note: at time of writing this model was still under development*) at N48 resolution, in comparison with observations and with the previous model version, HadAM3. The mean tropical climate is examined briefly first, before concentrating on four particular aspects: (1) the Asian summer monsoon; (2) the Madden-Julian Oscillation; (3) tropical winds; (4) variability of tropical convection. These four aspects cover a range of spatial and temporal scales, allowing an overall evaluation of the model's tropical performance to be made.

2. Mean tropical climate

Figure 1(a) shows the mean rainfall distribution in December-February (DJF) from a 17-year run of HadGAM1 (N48), and Fig.s 1(b to d) compare this with HadAM3 and the CMAP observed climatology. In HadGAM there is an increased dry bias over Indonesia compared with HadAM3, but errors over the subtropical oceans and the tropical Atlantic and Pacific are reduced slightly. In common with HadAM3, the Hadley circulation is overly strong, although it is weaker than in HadAM3, particularly in DJF. In June-August (JJA), the meridional circulation is narrowed and more concentrated at the equator. This is associated with including the new convection scheme in HadGAM1.

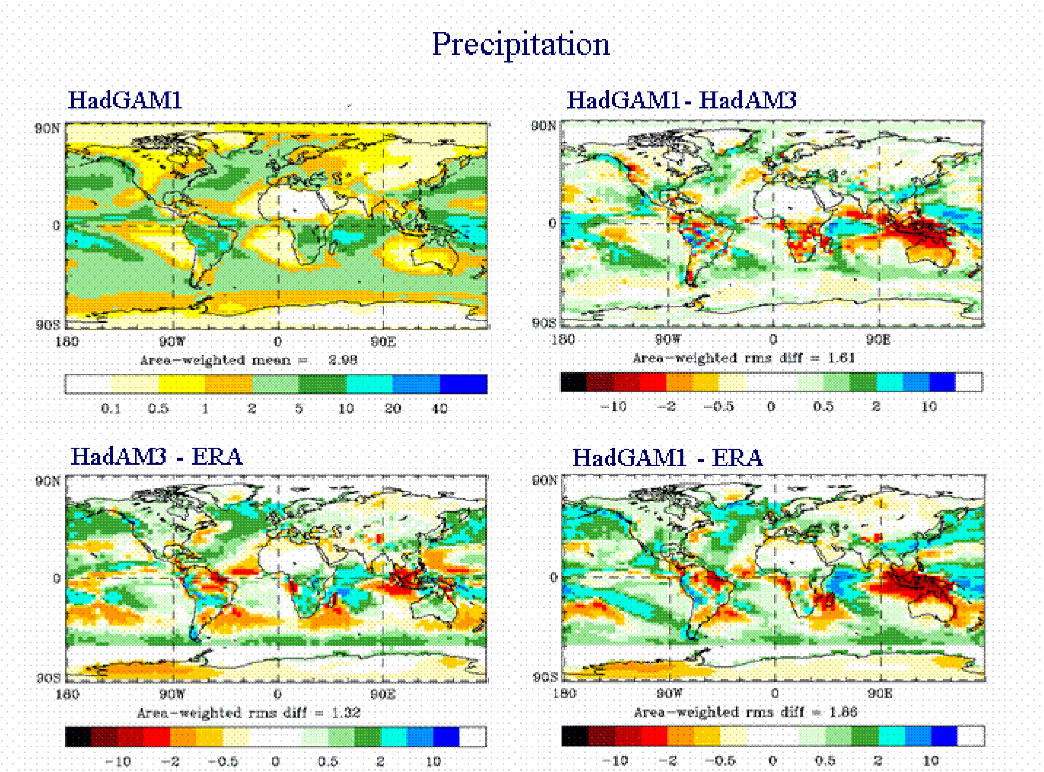

Figure 1: Precipitation in HadGAM1 and HadAM3 compared with CMAP (not ERA) observations

3. Asian Summer Monsoon

One of the major components of the tropical circulation is the Asian Summer Monsoon (ASM), on which the economies and livelihood of the populations of India and southeast Asia depend heavily. Simulation of this system and its variability remains a significant challenge for many GCMs. Previous versions of the Hadley Centre climate model have produced a reasonably good simulation of the ASM, although the monsoon strength, in terms of both circulation and precipitation, is rather overestimated, and the onset is slightly early in comparison with observations.

The monsoon climatology in HadGAM improves on HadAM3 in terms of the circulation strength (see Fig. 2), and in some aspects of the precipitation distribution, such as over the eastern equatorial Indian Ocean and over the west Pacific. However, the westerly low-level monsoon jet extends too far eastwards across East Asia, and precipitation is underestimated over India and over Indonesia.

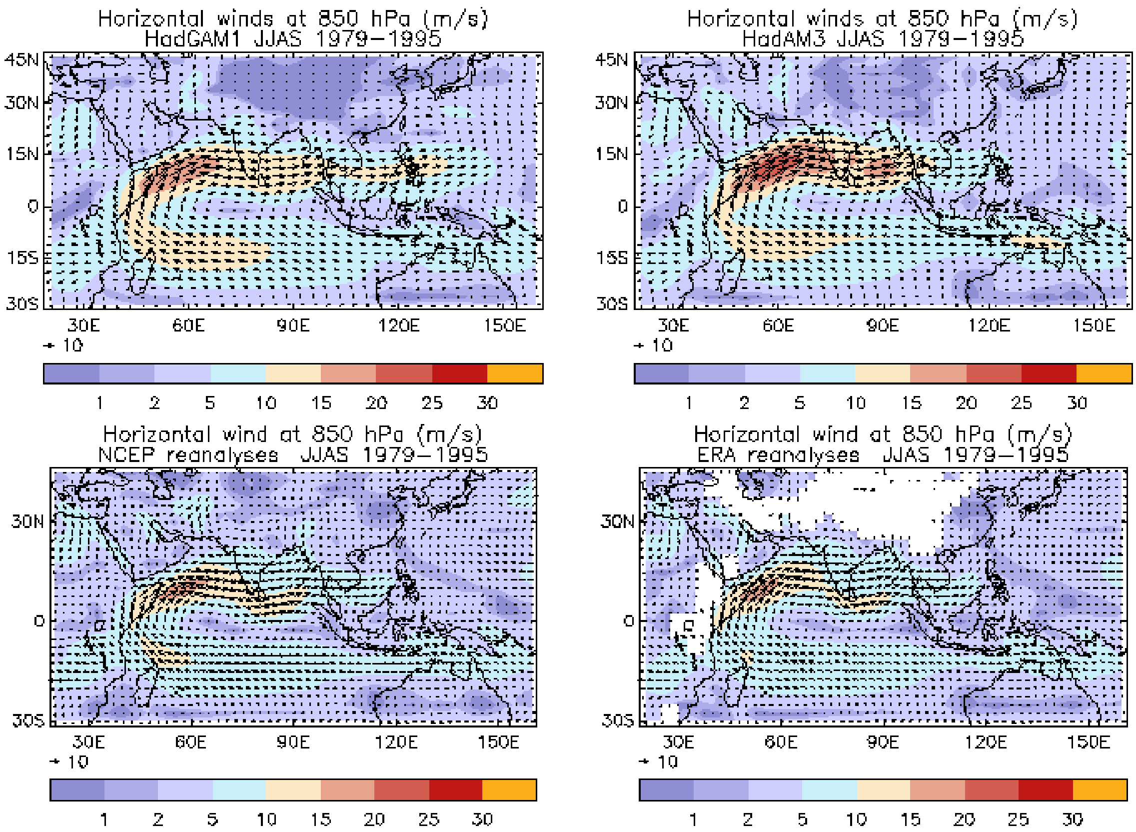

Figure 2: Horizontal winds at 850 hPa in HadGAM1, HadAM3 and two reanalysis datasets

Both atmosphere-only models have a dominant mode of interannual variability which explains of order 40% of the variance, higher than is observed. Despite the vast differences between the two models, their dominant modes are rather similar (Fig. 3). Easterly 850 hPa wind anomalies across East Asia and most of the Indian peninsula are associated with decreases in precipitation here, while increased convergence over Indonesia, western India and the Arabian Sea is associated with increased precipitation there. This dominant mode resembles that calculated by Molteni et al. (2002) from the NCEP/NCAR reanalyses, although in that case there is an additional contribution from the eastern equatorial Indian Ocean. Similar analysis of the coupled models, HadGEM and HadCM3, also shows the presence of these anomalies, suggesting an improved representation of the Indian Ocean SST dipole mode when the atmosphere and ocean are allowed to interact. A test of running HadAM3 with the SSTs from 20 years of

HadCM3 (Hilary Spencer, CGAM) shows a dominant mode of variability which is more similar to that of HadAM3 than indicating that the changes in HadCM3 are associated, at least in part, with the coupling rather than the SST errors.

HadAM3 shows significant teleconnections between the dominant mode of interannual variability and SSTs in the central and eastern Pacific. Wind and precipitation anomalies in El Nino years are very similar to the dominant mode of variability in this model. These teleconnections are rather weak in HadGAM1, suggesting that internal variability may be prevalent in this model. However, anomalies in El Nino years in HadGAM1 are quite similar to those observed, suggesting that strong SST forcing can outweigh the internal variability on some occasions. In contrast, HadAM3 responds too strongly to both local and remote SST forcing, such that teleconnections with SST, and anomalies in El Nino years, are less realistic than in HadGAM1.

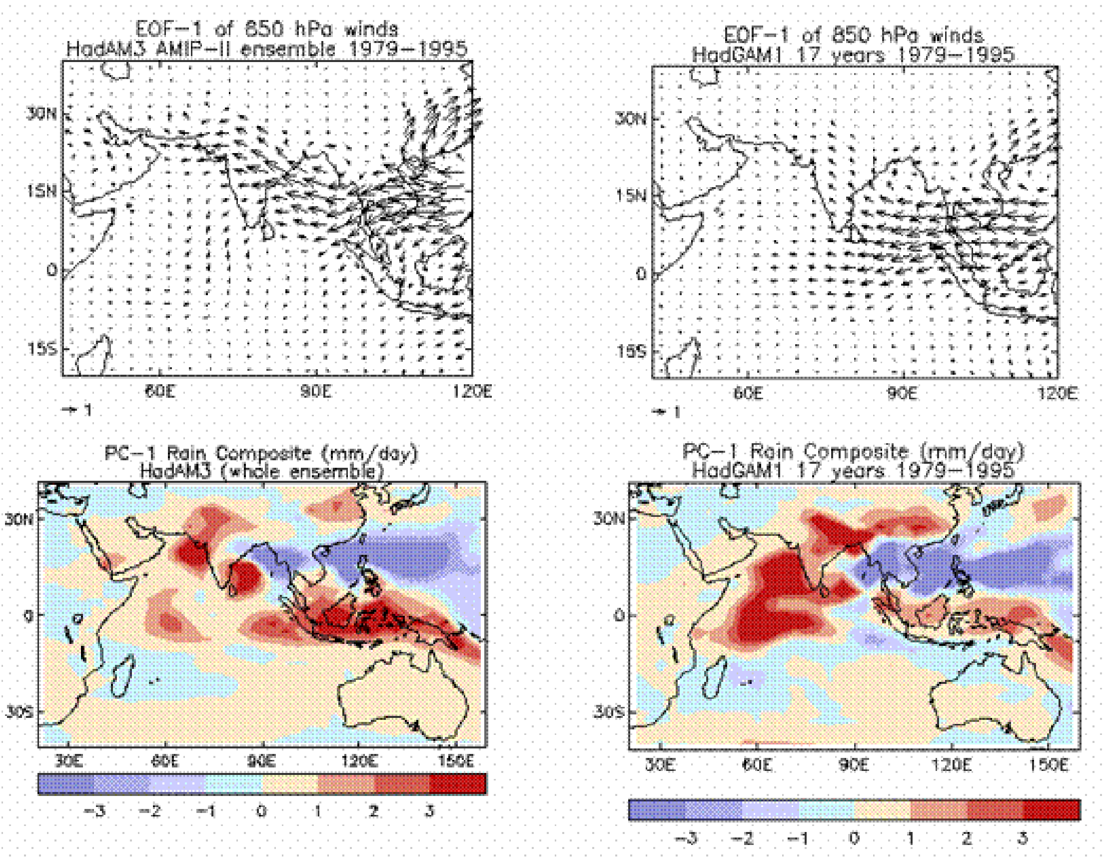

Figure 3: Dominant modes of interannual variability of 850 hPa winds in HadAM3 and HadGAM1

Analysis of the intraseasonal variability in the models shows a strong similarity between the dominant modes from the two models (Fig. 4), which describe around 12% of the variance in both cases. This mode is in good agreement with that calculated from NCEP reanalyses (Sperber et al, 2000), although in the reanalyses this mode is part of a series of patterns which describe the northward propagation of the Tropical Convergence Zone (TCZ). Northward propagation is harder to identify either of the models although more work is needed to investigate this properly.

It is noticeable that the intraseasonal and interannual modes resemble oneanother. The calculation of intraseasonal variability was made without removing the seasonal means from each year, so it includes the interannual variations. However, removing these has almost no impact on the patterns of variability, and merely reduces the variance explained to around 10%. Similarity between the dominant intraseasonal and interannual modes of monsoon variability has been noted in other GCMs and is also present in the observations.

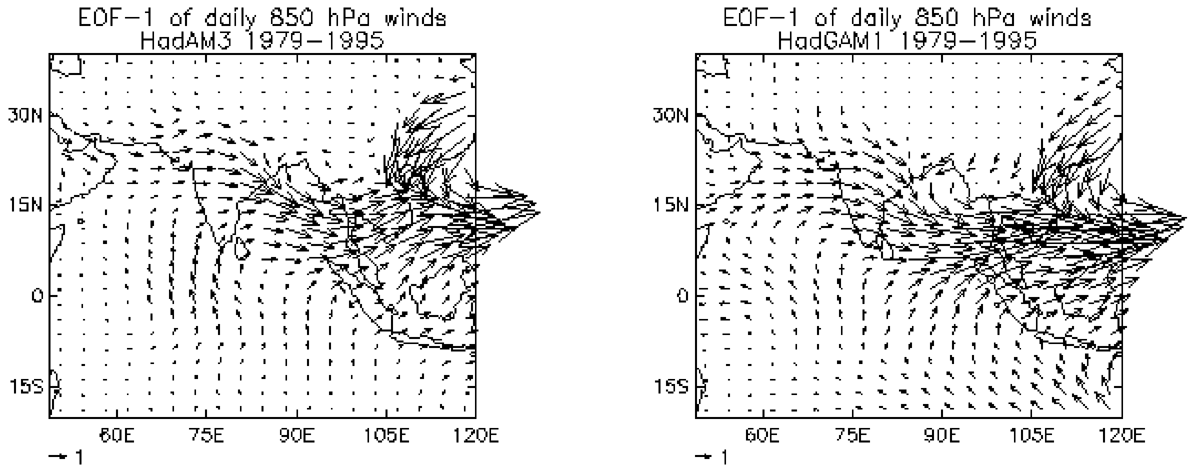

Figure 4: Dominant modes of intraseasonal variability of 850 hPa winds in HadAM3 and HadGAM1

This analysis shows that different atmosphere-only models can exhibit very similar dominant modes of interannual and intraseasonal variability, despite having rather different monsoon climatologies. However, in the case of HadAM3, the variability is strongly linked to SST forcing, while internal variability dominates in HadGAM. In spite of this, we find that strong SST forcing can outweigh the internal variability in HadGAM on some occasions.

4. The Madden-Julian Oscillation in HadGAM and HadGEM

The Madden-Julian Oscillation (MJO) is the major mode of variability of convection in the Tropics on timescales of 20-70 days. As well as modulating convective rainfall in the Tropics, the MJO may also influence extratropical weather through teleconnection patterns. Inness and Slingo (2003) discussed the simulation of the MJO in the coupled climate model HadCM3, and compared it to the MJO simulated in the atmosphere-only GCM HadAM3. Coupling the ocean and atmosphere was found to be an important element in improving the simulation of the MJO, but even in the coupled model, the MJO-related variability was too weak and the eastward propagation of convection did not extend into the West Pacific as observed. A preliminary analysis of the MJO simulated by HadGAM and HadGEM has now been undertaken.

4.1 The MJO in HadGAM (N48)

The simulation of the MJO in HadGAM is similar to that in HadAM3. Instead of representing a region of enhanced convection which propagates eastward across the Indian Ocean, Maritime Continent and West Pacific, the intraseasonal variability in both HadAM3 and HadGAM is dominated by a standing oscillation with centres in the Indian Ocean and West Pacific. Figure 5 shows the lag correlation of 20-100 day filtered OLR averaged between 10^{o}N and 10^{o}S with 20-100 day band-pass filtered 200 hPa velocity potential at 90^{o}E, also averaged between 10^{o}N and 10^{o}S for observations, HadAM3 and HadGAM. Neither GCM shows the eastward propagating signal seen in observations. Inness and Slingo (2003) showed that the lack of eastward propagation of convection in an atmosphere-only GCM was at least partly related to the lack of coupling between convection and SST. Therefore the lack of eastward propagation of convection in HadGAM is not surprising. However, In HadGAM, the variability of convection near the equator on intraseasonal timescales is generally stronger than in HadAM3 (i.e. closer to observed values). HadAM3 shows a distinct equatorial minimum through the Indian Ocean and West Pacific, which is no longer apparent in HadGAM, although the variance of OLR in HadGAM is still somewhat weak in the eastern Indian Ocean.

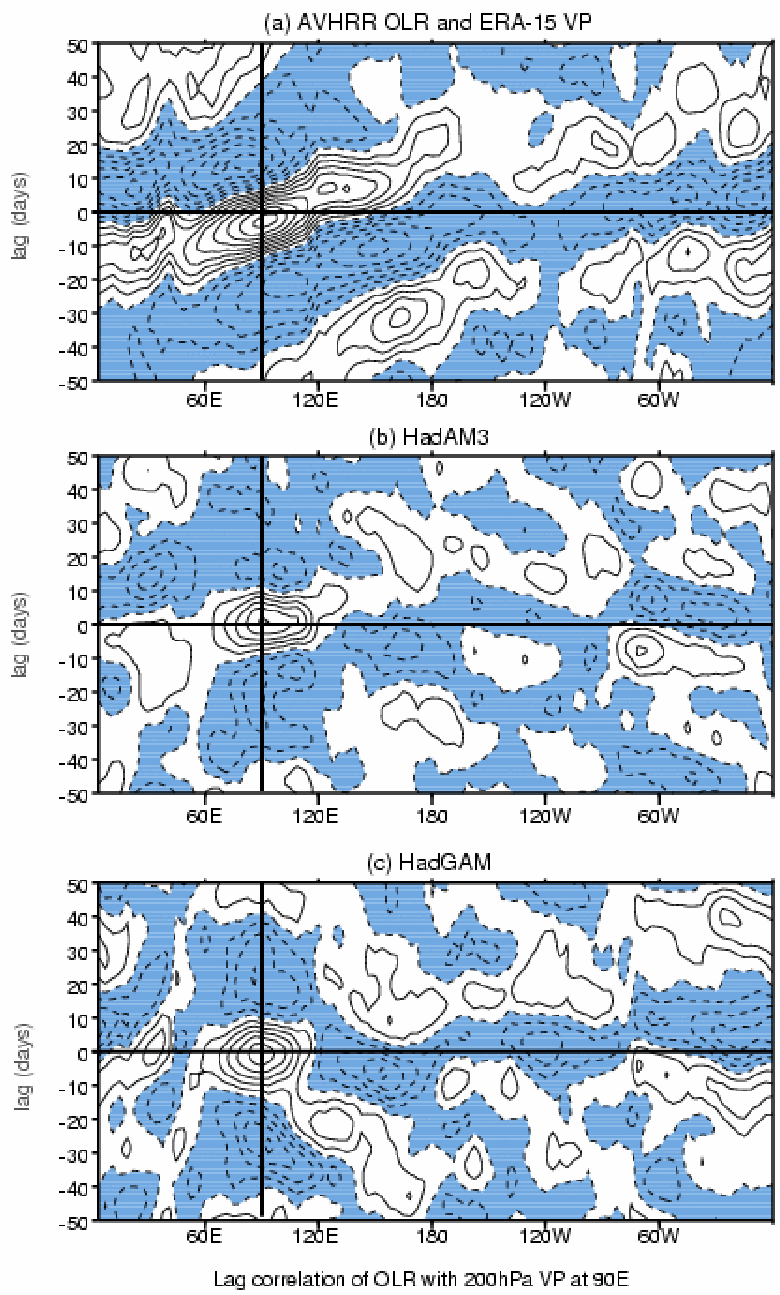

Figure 5: Lag-correlations of OLR averaged between 10°N and 10°S with 200 hPa velocity potential at 90°E, also averaged between 10°N and 10°S. Band-passed filtered to retain variability between 20 and 100 days. (a) Satellite observed OLR (NOAA AVHRR) and ECMWF re-analysis 200 hPa velocity potential, (b) HadAM3, (c) HadGAM.

4.2 The MJO in HadGEM (N48)

As with the previous generation of Hadley Centre climate models, the coupled GCM HadGEM represents the eastward propagation of MJO convection across the Indian Ocean and Maritime Continent which is not captured by the atmosphere-only component. Figure 6 is the same as for fig. 5 but for the two coupled GCMs HadCM3 and HadGEM. Both GCMs produce an eastward propagating signal in convection, but the propagation does not extend to the date-line, stopping instead at around 150°E. Inness *et al.* (2003) showed that this was related to basic state errors in the coupled model, specifically the lack of low level westerly winds on and to the south of the equator between the Maritime Continent and the date-line. Both HadCM3 and HadGEM have similar systematic errors in this region and so the eastward propagation of convection in this region is inhibited in both models.

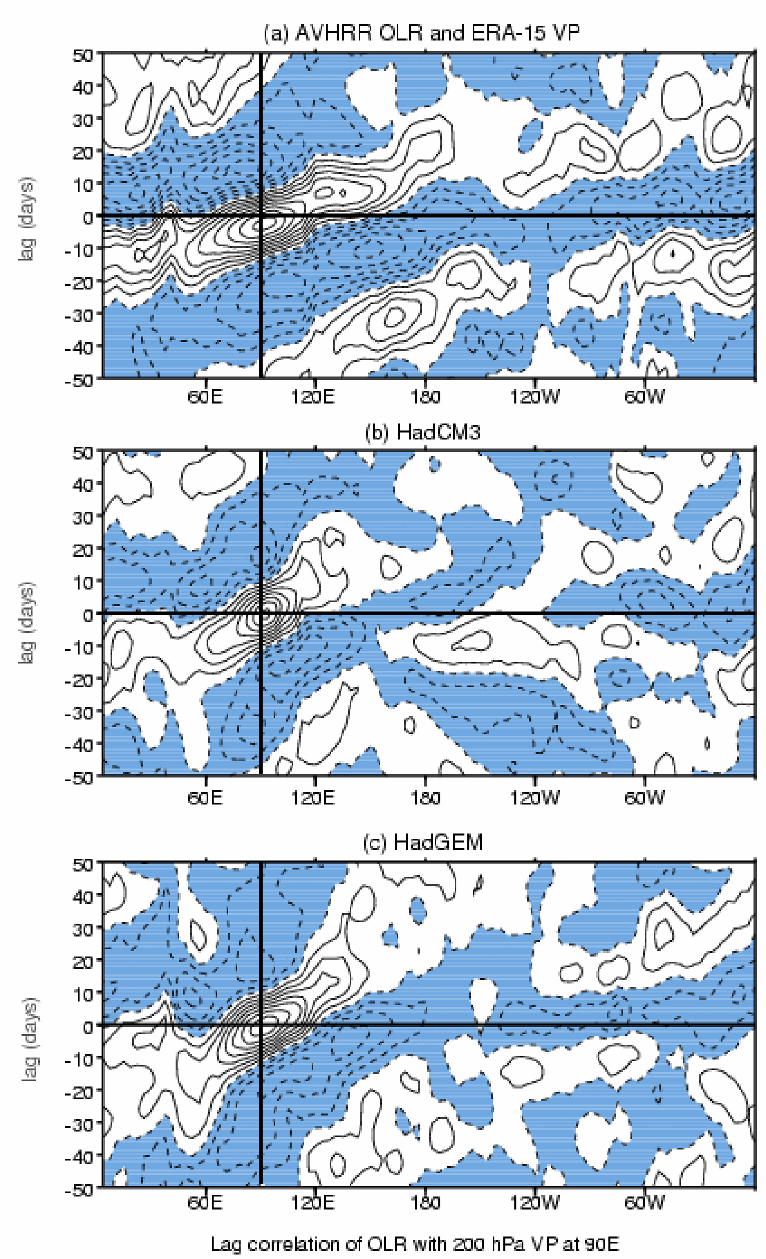

Figure 6: As Fig.5 but for (c) HadGEM.

The variance of convective activity around the equator in the Warm Pool region at intraseasonal timescales is higher in HadGEM than HadCM3, consistent with the increase in HadGAM described above. This is also apparent when looking at individual MJO events. Figure 7 shows time-longitude plots of 20-100 day filtered OLR anomalies for a single year from observations (1987-88) and the 2 coupled GCMs. The OLR anomalies in HadCM3 are rather weak and it is difficult to identify periods of coherent MJO activity. HadGEM produces several eastward propagating events between October and March, which are comparable in magnitude to those in the observations. However, studying individual MJO events in HadGEM also indicates several deficiencies in the MJO simulation. The propagation speed of the eastward moving convection seems to be slower than observed, and there are also a number of periods of westward propagation apparent, particularly in the West Pacific.

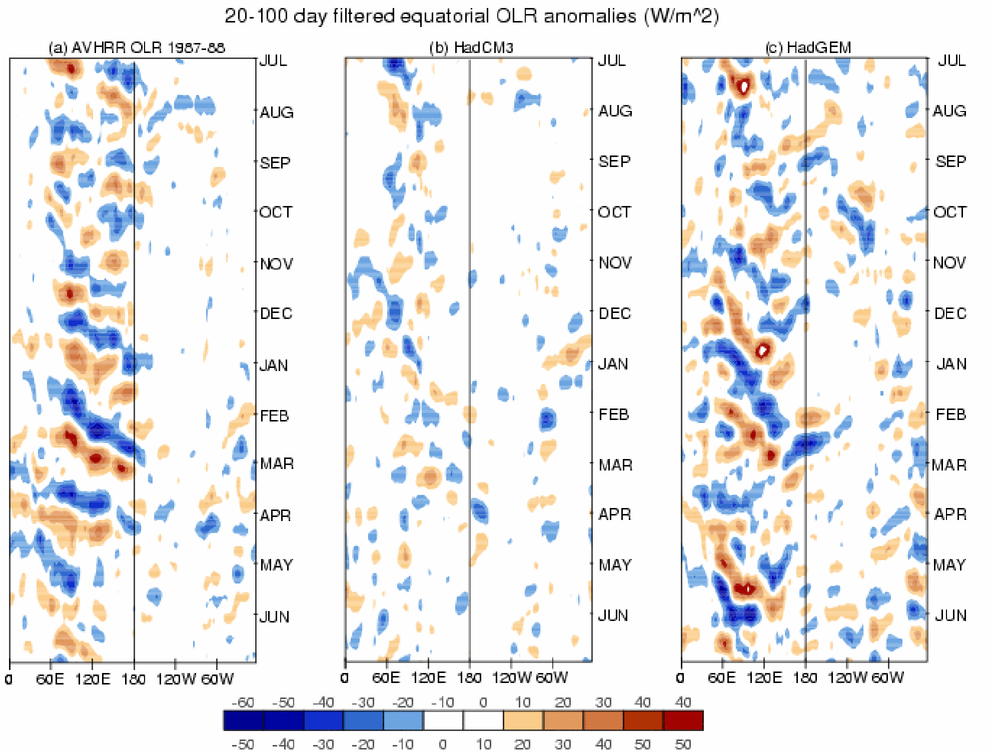

Figure 7: Time-longitude plots of 20-100 day band-pass filtered OLR anomalies averaged between 10°N and 10°S for 1 year (July-June). (a) NOAA AVHRR OLR 1987-88 (an active MJO season), (b) HadCM3, (c) HadGEM

5. Equatorial Indo-Pacific low level winds

The strength of the surface winds in the equatorial Pacific basin is a crucial element of the coupled climate system. The meridional sea-surface temperature gradient and sub-surface ocean temperature structure are intimately related to the surface wind-stress forcing. In turn, the basic state of the surface winds and upper ocean temperature structure are critical in determining the strength and frequency of El Niño events, the major mode of interannual climate variability (Fedorov and Philander, 2001). Thus a correct representation of the low level winds in the Pacific basin is a key element of the mean climate of an atmospheric GCM used for coupled climate modelling.

5.1 Comparison of winds with ECMWF re-analysis

Throughout the development of HadGAM/HadGEM, the surface winds and wind-stress in the Tropics have been closely monitored. In a coupled GCM, the winds across the equatorial Pacific will be set by coupled processes, so it is important that an atmosphere-only GCM, forced with realistic SSTs, can reproduce the observed winds reasonably closely.

Fig.8 shows the 1000 hPa zonal winds for October-April for ECMWF re-analyses (top), HadAM3 and HadGAM. Over the tropical oceans, the wind errors in HadAM3 and HadGAM are very similar. Both models have too strong easterly winds in the central and East Pacific, rather too strong westerlies in the West Pacific and a lack of westerly flow around the equator in the Indian Ocean. The main difference between the two model versions is that the westerlies in the West Pacific are slightly stronger in HadGAM. To a first approximation, this leads to enhanced low-level convergence near the date-line, and enhanced divergence over the Maritime Continent. This is associated with a reduction in precipitation over the Maritime Continent, with convection shifted to the east..

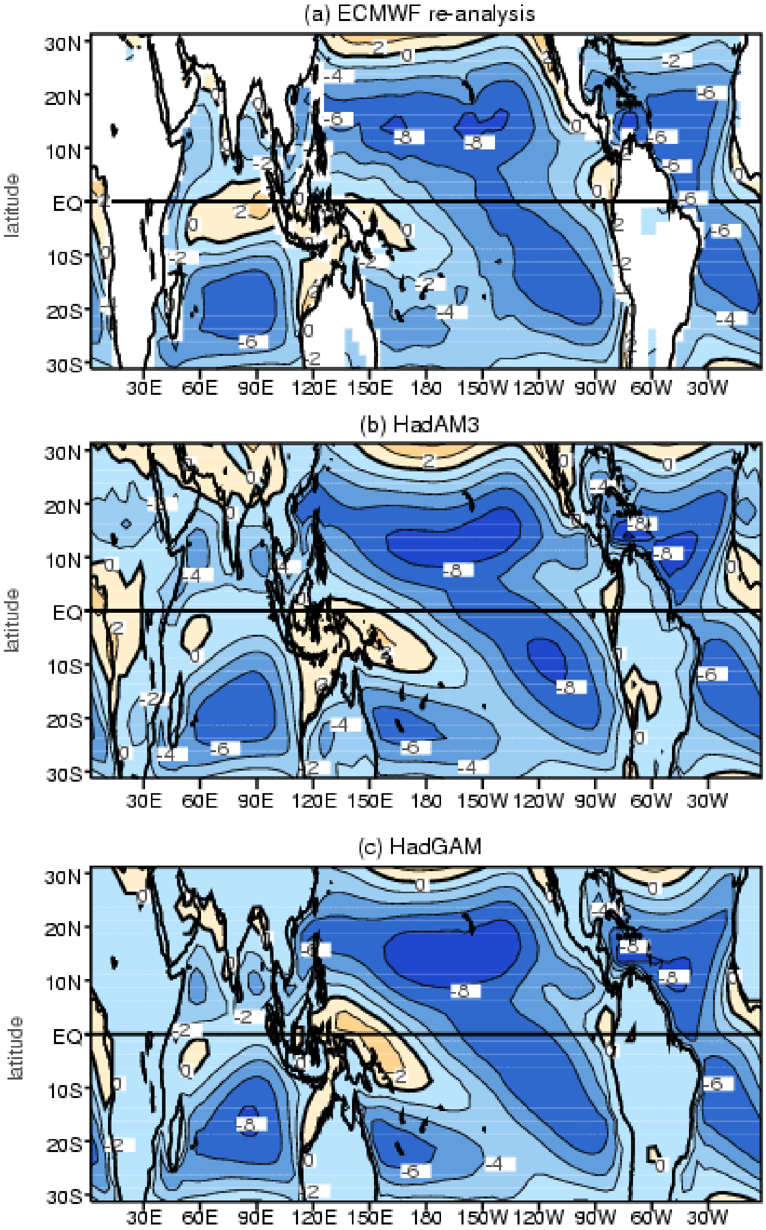

Figure 8: 1000 hPa zonal wind component for (a) ECMWF re-analyses, (b) HadAM3 and (c) HadGAM

In terms of the impact of the low level zonal winds on the Pacific Ocean SST structure in a coupled model, the strong easterly trades to the east of the date-line in both HadAM3 and HadGAM would be expected to induce colder than observed temperatures near the equator as the easterly wind anomalies will result in enhanced upwelling of cooler ocean water. Both models do indeed produce an equatorial Pacific SST cold tongue in coupled mode.

6. Temporal and spatial variability of tropical convection

Convectively coupled equatorial waves are a key part of the tropical climate system. A faithful representation of these wave modes is needed for predictions on all time-scales. However, at present there is little understanding of how well they are treated in state-of-the-art models and knowledge of these waves is very limited.

In a previous study (CGAM report on identifying and understanding model systematic errors:1999-2002), observed window brightness temperature and ERA-15 data have been used to diagnose convectively coupled equatorial waves and the results have been used as validation of the ability of standard (N48) and high resolution (N144) AMIP-II simulations with HadAM3 to represent the equatorial wave modes and their coupled behaviour. It is shown that convection in these models contains very limited variance coincident with equatorial wave modes. Although these models can simulate the dynamical aspects of equatorial waves, the coupling of these waves with convection, particularly in equatorial regions, is deficient.

To investigate convectively coupled equatorial waves in HadGAM, an initial step is to examine behaviours of convection in the model and compare them with those from observations. Here we will show some preliminary results from the OLR field. The data used are daily OLR for 1983 summer (May-Oct.) both from AVHRR observations and the HadGAM integration.

Figure 9(a,b) shows the seasonal mean and total standard deviation of observed and modelled OLR. It is clear that in non-convective regions modelled OLR is generally much higher than observed. In the convective region around Maritime continent and central America, modelled convection seems much weaker than observed. Figure 9(b) shows that a large standard deviation is generally coincident with convective regions both for observed and modelled OLR. However, modelled variability is much larger than observed, with its peak about twice that of observed.

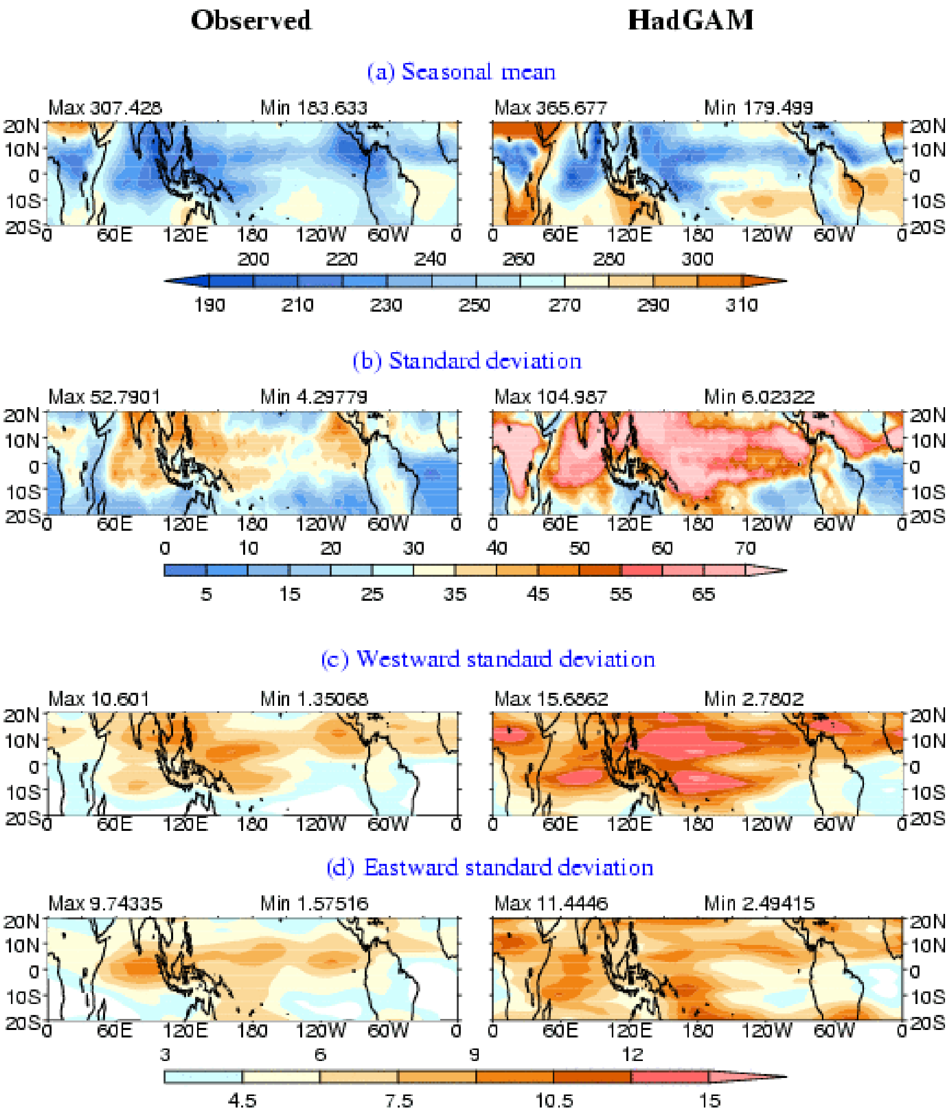

Figure 9: (a) Seasonal mean, (b) total standard deviation, and (c) westward and (d) eastward moving standard deviation of observed AVHRR OLR (left panels) and HadGAM OLR (right panels) for 1983 summer (May-October). Unit is Wm^{-2}.

A number of studies have shown that a substantial fraction of large scale variability in convection at timescale less than 30 days is associated with equatorial waves. Convection is then separated into westward and eastward moving components in a zonal wave number-frequency domain with k=2~10 and period=3~30 days. The standard deviation for westward and eastward moving components is shown in Fig.9(c,d), respectively. For westward moving convection, the model shows a larger variability than observations, similar to that for the total standard deviation. For eastward moving convection, observed large variability is mainly centred on the equator; whereas modelled variability is less confined on the equator although it is larger than observations again on average.

Space-time spectral analysis is then performed on the OLR data. Figure 10(a) shows the space-time spectra, averaged between 20°N and 20°S, for observed and modelled OLR. As expected, the modelled OLR has stronger power than observed. However the former is more like white-noise and seen everywhere; whereas the latter is more organised on a specified wavenumber-frequency domain and the power associated with eastward moving Kelvin waves can be seen (see Fig. 10(b) Kelvin wave dispersion curve).

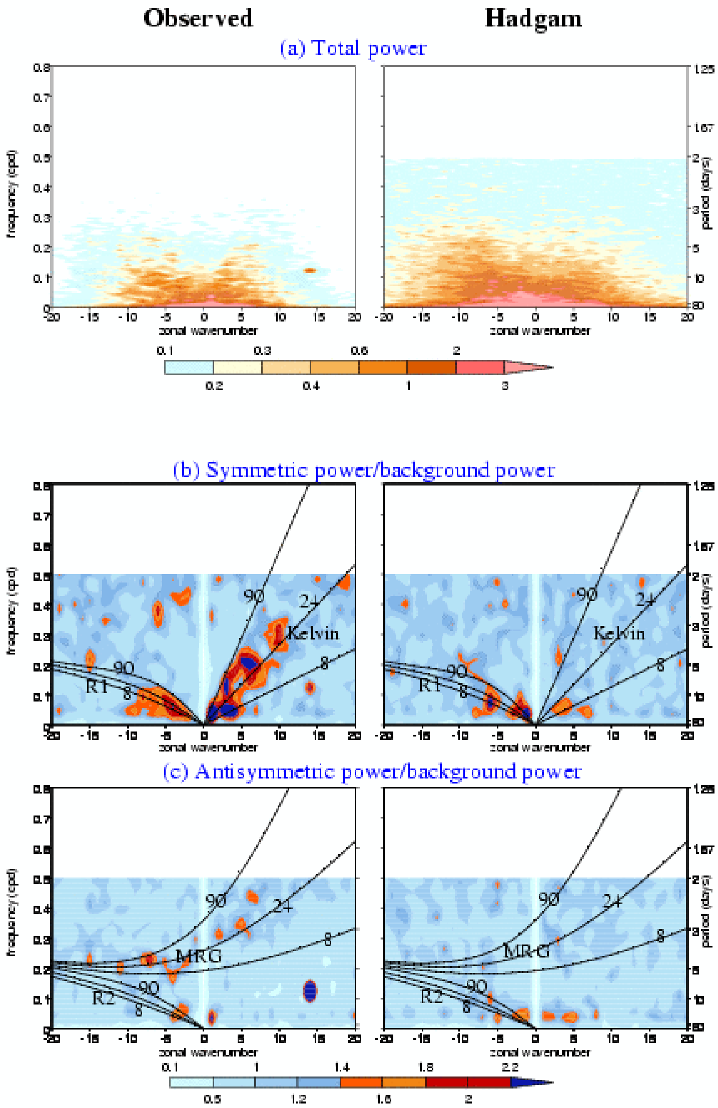

Figure 10: Zonal wavenumber-frequency power spectra of observed AVHRR OLR and HadGAM OLR for 1983 summer. (a) total power, (b) symmetric and (c) antisymmetric (about the equator) components divided by background power. Left and right panels are for observation and model respectively. The power has been averaged over the latitudes 20°N-20°S. Background power is calculated by smoothing the total power many times with a 1-2-1 filter in both frequency and wavenumber. Superimposed thin lines in (b) and (c) are the dispersion curves of equatorial Kelvin, *n*=1,2 Rossby (R1, R2) and mixed Rossby-gravity (MRG) waves for the equivalent depths of h=8, 24 and 90m. The curves have been Doppler-shifted with a 3 ms^{-1} easterly basic state.

To show to what extent the variability in Fig.9 is associated with equatorial waves, Figure 10(b,c) further gives the symmetric and antisymmetric power spectra, in which the background red spectrum has been removed to emphasise the preferred space and timescales of tropical convection, and the theoretical dispersion curves for equatorial wave modes are included for a range of typical equivalent depths. It is clearly demonstrated that observed tropical convection is organised on preferred space and time scales which coincide with various theoretical equatorial waves modes (equatorial Rossby (R), mixed Rossby-gravity (MRG) and Kelvin waves). In contrast, the model contains very limited variance coincident with these equatorial wave modes. Although there is variance associated Rossby waves, variance related to equatorial Kelvin and MRG waves is almost entirely absent from the model. This model deficiency is similar to that for HadAM3.

Future work will investigate coupling features of equatorial waves with tropical convection in the HadGAM, in which 1992 summer data will be used for comparing with results from observation and HadAM3.

7. Summary

Several aspects of the tropical performance of HadGAM/GEM1 have been assessed, covering a range of spatial and temporal scales. In some aspects, HadGAM/GEM improves on HadAM/CM3. The positive bias in the Hadley circulation is reduced and some areas of the precipitation climatology are improved. The Asian summer monsoon circulation is closer to climatology, and wind and precipitation anomalies in El Nino years are similar to those observed, despite the finding that interannual variability in this model may be dominated by internal variations. This contrasts with HadAM/CM3 which responds too strongly to both local and remote SST forcing. Intraseasonal variability of convection near the equator is generally stronger and closer to observations, and HadGEM produces several eastward-propagating events with comparable magnitude to observations.

There are aspects of tropical performance where similar errors are seen in both model versions, e.g. in the spatial and temporal distribution of convection; the spatial pattern of tropical intraseasonal variability in the atmosphere-only models and the limited extent of eastward propagation in the coupled models due to the systematic error in low-level westerly winds; the limited variance coincident with the equatorial Rossby, MRG and Kelvin wave modes. Where the errors are associated with coupled atmosphere-ocean phenomena, the errors tend to be larger in the atmosphere-only models.

Past experience of model development has shown that the tropical performance is very robust and difficult to improve. The area of the model on which it depends most strongly is the convection scheme. Despite the many changes made to the convection scheme in HadGAM/GEM, it is still largely a mass-flux scheme. The errors we see are common to other GCMs, which also use this type of parametrisation. Work is already underway to design a turbulence-based convection scheme which may, at least, change the pattern of errors. Other aspects of the model which also contribute to the tropical performance include the cloud scheme and the treatment of cloud anvils detraining from the top of deep convection, the diurnal cycle of convection over land and the complex circulation patterns generated by land-sea contrasts, and the horizontal and vertical resolution. In the coupled model, the treatment of the ocean mixed layer and the atmosphere-ocean coupling are also important. Many of these aspects are already being tackled, using HadGEM as a basis. The improvements made to this model over HadAM3/CM3 provide a more solid framework for developing the next generation of climate models.

Acknowledgements
This work was done under the Government Meteorological Research contract. The development of HadGAM1/GEM1 involved the efforts of a large number of people, to whom the authors are indebted,

References

Fedorov, A. V. and Philander, S. G., 2001. A stability analysis of tropical ocean-atmosphere interactions: bridging measurements and theory for El Niño. J. Clim., **14**, 3086-3101.

Inness, P.M. and J.M. Slingo, 2003. Simulation of the Madden-Julian Oscillation in a coupled general circulation model I: Comparison with observations and an atmosphere-only GCM. *Journal of Climate*, **16**, 345-364.

Inness, P.M., J.M. Slingo, E. Guilyardi and J. Cole, 2003. Simulation of the Madden-Julian Oscillation in a coupled general circulation model II: The role of the basic state. *Journal of Climate*, **16**, 365-382.

Molteni, F., S. Corti, L. Ferranti and J.M. Slingo, 2002. Predictability experiments for the Asian summer monsoon: impact of SST anomalies on interannual and intraseasonal variability. *J. Clim.* **16,** 4001-4021

Sperber, K.R., J.M. Slingo and H. Annamalai, 2000. Predictability and the relationship between subseasonal and interannual variability during the Asian summer monsoon. *Q.J.R .Meteorol. Soc.*, **126**, 2545-2574.